PCCP

Kinetic studies of the gas phase INO_2 self-reaction

Kate S. Gawler, Gavin Boakes and David M. Rowley*

Department of Chemistry, University College London, Christopher Ingold Laboratories, 20 Gordon St., London, UK WC1H 0AJ

Received 4th April 2003, Accepted 10th July 2003
First published as an Advance Article on the web 30th July 2003

Flash photolysis of $CF_3I/NO_2/N_2$ gas mixtures has demonstrated the presence of the INO_2 self-reaction:

$$INO_2 + INO_2 \rightarrow I_2 + 2NO_2 \quad (1)$$

The occurrence of reaction (1) has been confirmed through simultaneous monitoring of NO_2 and I_2 by time-resolved UV-visible absorption spectroscopy. The second order rate coefficient for reaction (1), k_1, has been measured and the first temperature dependence study of k_1 has been carried out. A positive temperature dependence for k_1 was observed between 277.7 and 344.8 K which is described by $k_1(T) = (4.7 \pm 0.55) \times 10^{-13}$ $\exp((-1670 \pm 340)/T)$ molecule^{-1} cm^3 s^{-1}. Errors are 2σ. The atmospheric implications of these results are briefly discussed.

Introduction

The role of iodine in atmospheric ozone destruction has been of increasing interest since the 1980's.[1–6] It is now recognised that the principal sources of atmospheric iodine are alkyl iodides of biogenic origin released from the sea. The most abundant of these in the atmosphere is methyl iodide, CH_3I,[7–10] although other iodocarbons, including CH_2I_2, CH_2IBr and CH_2ICl have also been observed in marine regions.[11–13] Solar photodissociation of CH_3I and other alkyl iodides releases I atoms which can react with O_3, destroying it. Reactions which then reconvert IO free radicals to I atoms, either directly or indirectly, can complete a catalytic cycle for ozone loss, such as

$$I + O_3 \rightarrow O_2 + IO \quad (2)$$

$$IO + NO \rightarrow I + NO_2 \quad (3)$$

The extent of iodine catalysed atmospheric ozone destruction is dependent upon the amount of gas phase iodine present and the partitioning between the halogen's source gases, 'active' species (I and IO) and 'reservoir' forms. Active forms can participate in ozone destroying reactions while the formation of reservoirs mediates ozone loss until the halogen is re-released by reactive or photolytic processes.

In comparing iodine with its lighter halogen counterparts it is found that the atmospheric lifetimes of iodine source gases with respect to solar photodissociation are short (of the order of seconds to minutes). This can be explained by considering two factors: first the notably weaker C–I bond compared to its C–Br and C–Cl analogues[14] and second that iodocarbons typically absorb in the UV-visible region, whereas the chloro- and bromo-analogues typically absorb at shorter wavelengths where terrestrial solar flux is reduced. As a result iodine chemistry, including iodine catalysed ozone loss, is thought to be confined predominantly to the troposphere. However, considering the efficiency of iodine catalysed ozone loss, the formation of atmospheric iodine reservoir compounds is disfavoured compared to the other halogens. Moreover, the atmospheric stability of iodine reservoirs even when formed is likely to be low, and iodine is likely to be an efficient agent for ozone destruction on an atom for atom basis.

By analogy with other halogens, the principal reservoir species for atmospheric iodine are likely to be HI, HOI and $IONO_2$. HI and HOI are formed from the reaction of I and IO with HO_2 free radicals respectively.[15–17] $IONO_2$ is formed from the association of IO with NO_2:[16,18]

$$I + HO_2 \rightarrow HI + O_2 \quad (4)$$

$$IO + HO_2 \rightarrow HOI + O_2 \quad (5)$$

$$IO + NO_2 + M \rightarrow IONO_2 + M \quad (6)$$

Solar photolysis of HOI and $IONO_2$ re-releases I atoms or IO free radicals and may therefore itself comprise a catalytic ozone loss cycle in the troposphere.[19–21] The formation of INO_2 is another possibility in the atmosphere, reaction (7).[22]

$$I + NO_2 + M \rightarrow INO_2 + M \quad (7)$$

The subsequent fate of INO_2 is consequently of interest in characterising the atmospheric role played by this species.

The Cl and Br counterparts of INO_2 have been the subject of numerous studies. Like nitryl iodide, both nitryl chloride, $ClNO_2$, and nitryl bromide, $BrNO_2$, are formed in the gas phase *via* reaction with NO_2.[23–25] $ClNO_2$ and $BrNO_2$ are also formed in the marine boundary layer *via* the reaction of nitrogen oxides with sea salt aerosols, reaction (8), where X = Cl, Br.[26,27]

$$N_2O_5 + NaX \rightarrow XNO_2 + NaNO_3 \quad (8)$$

The XNO_2 species may also be formed in the upper troposphere and stratosphere by reaction of N_2O_5 with dissolved HX, reaction (9).[28,29]

$$N_2O_5 + HX \rightarrow XNO_2 + HNO_3 \quad (9)$$

Ab initio calculations on XNO_2 predict the structure to be planar with C_{2v} symmetry.[30] This symmetry has been observed for both $ClNO_2$ and $BrNO_2$ in high resolution FTIR studies.[31,32] XNO_2 is also thought to isomerise into *cis*-XONO and *trans*-XONO. These isomers have been predicted by *ab initio* calculations.[30,33] The absorption cross-section for $ClNO_2$ has been recorded using UV absorption spectroscopy[34] and resonance fluorescence to detect photolytically produced Cl atoms.[35] All three isomeric forms of $ClNO_2$ have been

 DOI: 10.1039/b303757f

observed using matrix isolation.[36] IR absorptions of $BrNO_2$ have been recorded as well as the UV absorption cross-section of *cis*-BrONO.[27,37] The *trans*-BrONO isomer has only been observed *via* matrix isolation together with the other two isomers.[38] Orlando and Burkholder[39] have carried out a FTIR study of $BrNO_2$ and have suggested that the *cis* and *trans* forms of the species are likely to isomerise into the more stable $BrNO_2$ form. However, *ab initio* calculations by Lee[33] have suggested that both $BrNO_2$ and *cis*-BrONO are stable enough to exist in the stratosphere. The isomerisation channel from $BrNO_2$ to BrONO has been studied theoretically by Yu *et al.*[40] INO_2 has been observed in the gas phase by FTIR and as part of a matrix isolation study.[41,42] No studies of the UV absorption spectrum of INO_2 have been reported, however, although estimates of the INO_2 cross-sections, based upon red-shifted $ClNO_2$ cross-sections have been used to estimate the solar photolysis rate coefficient for INO_2, giving $J_{INO_2} = 3.48 \times 10^{-4}$ s^{-1}.[43]

The photodissociation products of $ClNO_2$ have been studied at 350 nm by Nelson and Johnston.[35] In this study photolytically produced Cl and O atoms were monitored in order to assess which bonds broke on photolysis. These authors found that breakage of the N–Cl bond was the major photolytic channel, $\Phi = 0.93 \pm 0.15$, and N–O cleavage the minor channel, $\Phi \leq 0.02$. The photodissociation of gaseous $ClNO_2$ has also been investigated at 235 and 248 nm.[44,45] Both of these studies also find that production of Cl atoms is the dominant photolytic pathway. No direct studies of the photolysis products of gas phase $BrNO_2$ or INO_2 exist, although *ab initio* studies suggest that their photolysis produces halogen atoms.[46]

Previous kinetic studies of XNO_2 reactions are not extensive and are all summarised in Table 1. Kinetic studies of $ClNO_2$ have shown it to react with Cl, NO and OH.[35,47,48] Reaction with NO and OH are too slow to exert any significance under atmospheric conditions. $BrNO_2$ is known to react with Br in a rapid reaction and with NO but the latter is too slow to have any atmospheric significance.[39,49]

To date there are very few studies on nitryl iodide, INO_2, despite it being suggested as a reservoir for iodine in the troposphere.[50] Unlike its lighter halogen analogues there has been no evidence reported for the formation of INO_2 *via* heterogeneous reactions. As a result INO_2 is thought to form solely *via* the gas phase reaction of I and NO_2, (7).[22,24,51–53]

INO_2 is reported to self-react, and to react with I atoms.[22] However, only a single kinetic study of the INO_2 self-reaction exists reporting a 350 K rate coefficient of $k_1 = 1.66(+1.65)(-0.83) \times 10^{-14}$ molecule^{-1} cm^3 s^{-1}.[22] With this rate coefficient, and with the probable low concentrations of atmospheric INO_2, self-reaction of INO_2 is unlikely to compete with solar photolysis as an atmospheric sink of INO_2. However, since the temperature dependence of the INO_2 self-reaction has not been previously studied, and since the INO_2 photolysis rate is an estimate, further quantification of both of these potential loss mechanisms is warranted.

Table 1 Reactions of XNO_2 (X = Cl, Br, I)

Reaction	k (298 K)/ molecule^{-1} cm^3 s^{-1}	Reference
$ClNO_2 + Cl \rightarrow Cl_2 + NO_2$	5.50×10^{-12}	35
$ClNO_2 + NO \rightarrow NOCl + NO_2$	1.20×10^{-17}	47
$ClNO_2 + OH \rightarrow HOCl + NO_2$	3.50×10^{-14}	48
$BrNO_2 + Br \rightarrow Br_2 + NO_2$	$10^{-10} > k > 10^{-11}$	39
$BrNO_2 + NO \rightarrow BrNO + NO_2$	1.74×10^{-15}	49
$INO_2 + I \rightarrow I_2 + NO_2$	8.32×10^{-11} [a]	22
$INO_2 + INO_2 \rightarrow I_2 + 2NO_2$	1.66×10^{-14} [b]	22
$INO_2 + INO_2 \rightarrow I_2 + 2NO_2$	$(1.50 \pm 0.53) \times 10^{-15}$ [c]	This work

[a] At $T = 330$ K. [b] At $T = 350$ K. [c] At $T = 303$ K.

In this work, the regeneration of I_2 and NO_2 following flash photolysis of CF_3I/NO_2 mixtures has been attributed to the self-reaction of INO_2 and the kinetics of this process have been investigated.

Experimental

The apparatus used has been described elsewhere in detail[54] therefore only a brief description is given here. Gas mixtures prepared using calibrated mass flow controllers were flowed continuously through a cylindrical thermostatted quartz vessel 98.2 cm in length. Gas phase reactions were initiated by a short duration (20 μs) intense photolytic pulse from a 1 m long, xenon flashlamp (500 J pulse^{-1}) situated adjacent and parallel to the reaction vessel. Temporal evolution of species concentration during the course of an experiment was monitored using UV-visible absorption spectroscopy. The source for absorption measurements was a 75 W xenon arc lamp (Hamamatsu), output from which was collimated along the length of the reaction vessel. Light transmitted through the reaction vessel was focused onto the entrance slit of a 0.25 m, 300 g mm^{-1} diffraction grating Czerny-Turner spectrograph (Chromex) and wavelength resolved across the top 30 rows of a 2-dimensional 298 column × 1152 row pixel array charge-coupled device (CCD) detector (Wright Instruments Ltd.). The CCD converted incident light into photocharge, and thus recorded a transmission spectrum of the gas mixture. The process of row-by-row charge transfer across the detector in the axis perpendicular to the spectral axis was used to record sequential, time resolved spectra of the gas mixture before, during and after photolysis. Post-photolysis absorbance spectra were calculated relative to pre-photolysis intensities using Beer's law. Consequently, absorbance spectra exhibited changes in absorbance resulting from the photolysis flash and subsequent chemistry. UV-visible absorbing species in the reaction vessel were monitored by fitting reference (absorption cross-sections × optical pathlength) to observed absorbance spectra obtained at each time point. For spectrally structured absorption cross-sections, in this case NO_2, 'differential' fitting ensured that unequivocal monitoring of the absorbing species was achieved. This process involved the high pass filtering of the experimentally observed absorption spectra along with identical filtering of the NO_2 reference cross-sections. Since the reference cross-sections are strictly dependent on the instrumental resolution used, the high resolution reference NO_2 cross-sections used in this work[55] were smoothed to the instrumental resolution adopted in this study (0.22 nm FWHM) using a rectangular sliding averaging kernel. The spectral region monitored in these experiments was typically $\lambda = 390$–450 nm, where NO_2 absorption cross-sections maximise. 1000 × 1 ms duration transmission spectra were typically recorded in an experiment, with photolysis initiated after 300 ms. CF_3I (99%, Fluorochem, used as supplied)/NO_2 (99.9% purity, mixed to 1.05% in helium, BOC, used as supplied)/N_2 (99.99%, BOC, used as supplied) mixtures used in the photolysis experiments contained initial concentrations of CF_3I in the range $(4$–$8) \times 10^{17}$ molecule cm^{-3} and NO_2 in the range $(1.5$–$2.5) \times 10^{15}$ molecule cm^{-3}, balanced by N_2 to 1 atmosphere. Time resolved species concentration *versus* time profiles were analysed to yield kinetic information.

Results and discussion

Photolysis of $NO_2/CF_3I/N_2$ mixtures demonstrated the loss of NO_2 from the gas phase. Fig. 1 shows a typical time-averaged (for 200 ms) post-photolysis spectrum clearly showing a negative contribution to absorbance (relative to pre-photolysis) with distinctive vibronic structure attributed to NO_2. Change

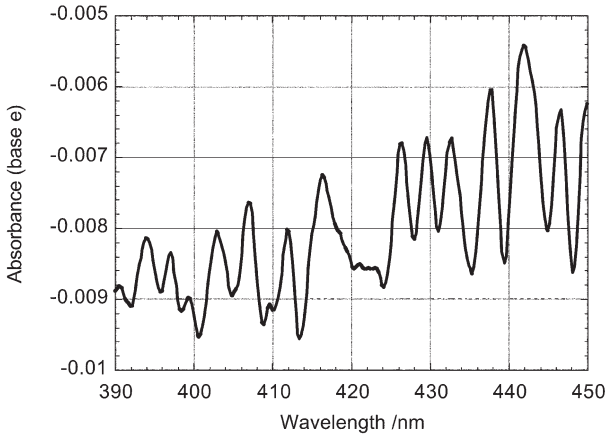

Fig. 1 Absorbance spectrum of a flash photolysed $NO_2/CF_3I/N_2$ gas mixture generated from 200 ms time-averaged post-photolysis intensities (I_t) relative to pre-photolysis intensities (I_0).

in NO_2 concentration was quantified using differential spectroscopy as described above. The least squares fit of the time-averaged high pass filtered reference and experimental spectra is shown in Fig. 2 indicating a near zero residual. The temporal evolution of NO_2 concentrations relative to pre-photolysis was obtained by repeating this spectral fitting for all 1000 sequential 1 ms spectra obtained before, during and after photolysis. The temporal evolution of the NO_2 concentration, recorded in both the presence and in the absence of CF_3I under identical conditions, is shown in Fig. 3(a). In Fig. 3(b), the temporal evolution of the NO_2 concentration is shown for experiments with three different starting CF_3I concentrations. Both figures indicate that in the presence of CF_3I, the initial loss of NO_2 is followed by some recovery in the NO_2 concentration (approximately half of the NO_2 initially lost). Moreover, the magnitude of the initially lost NO_2 concentration was in proportion to the initial CF_3I concentration employed. By contrast, no systematic variation of the NO_2 decay traces resulted from changing the initial NO_2 concentration over the range adopted. This behaviour was consequently attributed to CF_3I photolysis followed by the formation and subsequent self-reaction of INO_2, reaction (1).

$$CF_3I + h\nu(\lambda < 300\ \text{nm}) \rightarrow CF_3 + I \quad (10)$$

$$I + NO_2 + M \rightarrow INO_2 + M \quad (7)$$

$$INO_2 + INO_2 \rightarrow I_2 + 2\ NO_2 \quad (1)$$

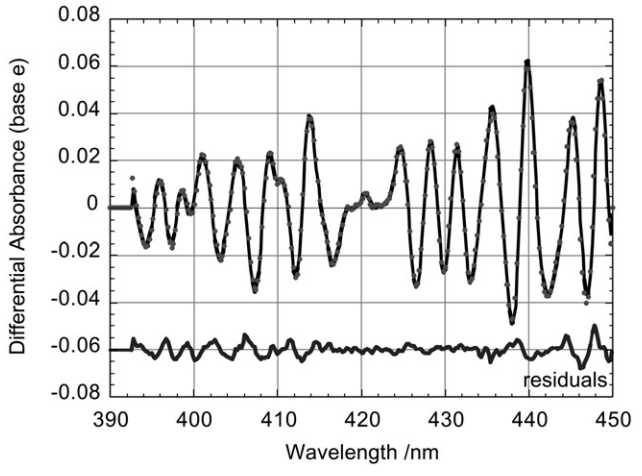

Fig. 2 High-pass filtered post photolysis absorbance spectrum (points) with identically filtered, fitted NO_2 reference spectrum (line) and residuals. Residuals have been offset by −0.06 absorbance units for clarity.

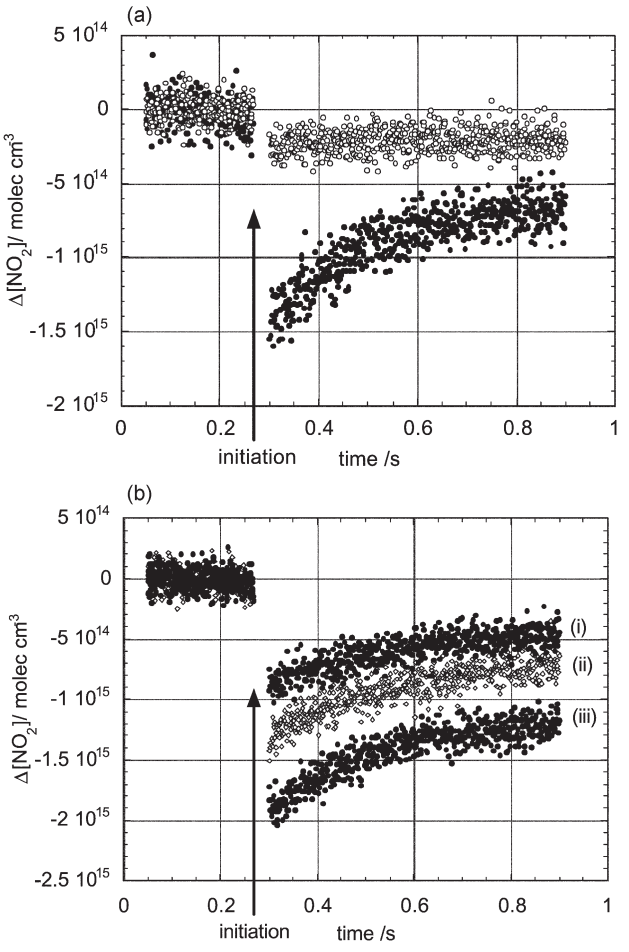

Fig. 3 (a) Temporal evolution of change in NO_2 concentrations in the photolysis of a $NO_2/CF_3I/N_2$ gas mixture (filled symbols). Temporal evolution of change in NO_2 concentrations in the photolysis of a NO_2/N_2 gas mixture (open symbols). In both cases, changes in $[NO_2]$ are calculated relative to pre-photolysis values. (b) Temporal evolution of change in NO_2 concentrations in the photolysis of $NO_2/CF_3I/N_2$ gas mixture at three different initial $[CF_3I]$: (i) $[CF_3I] = 2.35 \times 10^{17}$ molecules cm^{-3}, (ii) $[CF_3I] = 4.64 \times 10^{17}$ molecules cm^{-3}, (iii) $[CF_3I] = 7.80 \times 10^{17}$ molecules cm^{-3}.

To confirm the attribution of the INO_2 self-reaction, the residual post-photolysis spectra, following the removal of the (negative) absorbance contribution from NO_2, were inspected. Fig. 4(a) shows such a spectrum, which has a positive absorbance contribution increasing to higher wavelengths. This absorbance was attributed to the formation of molecular iodine, the reference spectrum of which is shown over the same wavelength range in Fig. 4(b).[56] Using the CCD, temporal monitoring of the I_2 residual spectrum was also carried out. The results from this are shown in Fig. 5. It was apparent that the recovery of NO_2 concentrations was accompanied by the formation of gas phase I_2, in a 2 : 1 stoichiometric ratio, consistent with the occurrence of reaction (1).

Having demonstrated the existence of the INO_2 self-reaction in this system, close consideration of any potentially complicating chemistry was undertaken prior to recording temperature dependent rate coefficients. Under the experimental conditions used (CF_3I in excess over NO_2), CF_3I photodissociation dominated that of NO_2. This was confirmed in experiments carried out in the absence of CF_3I which showed that the loss of NO_2 was far smaller than that observed with CF_3I present (Fig. 3(a)). Notwithstanding the low $[NO_2]$ employed here, the likely fate of the CF_3 radical produced in (10) is reaction with NO_2.[57,58] The principal products of the

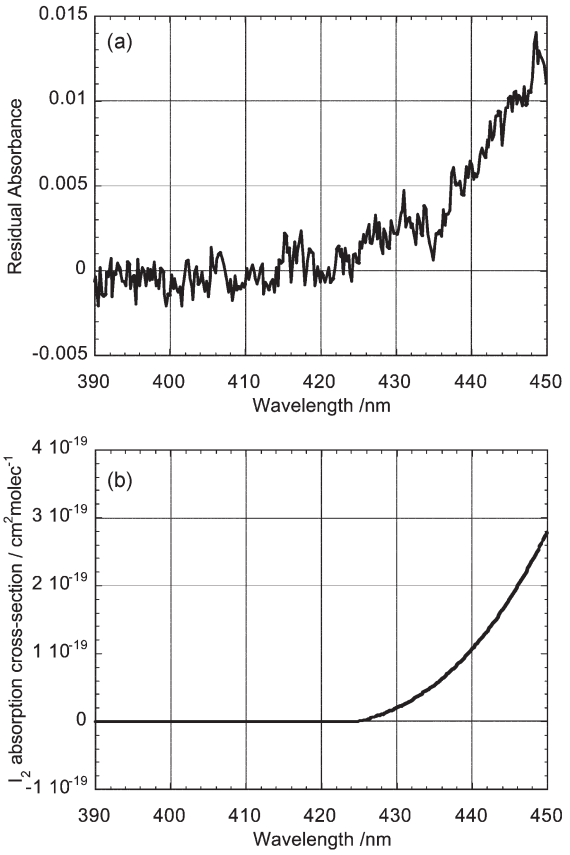

Fig. 4 (a) Residual absorbance following subtraction of the contribution of NO_2 to the absorbance spectrum of a photolysed $NO_2/CF_3I/N_2$ gas mixture. (b) Absorption cross-sections of I_2 over the same wavelength range as in (a).

$CF_3 + NO_2$ reaction, COF_2 and FNO, do not undergo further reaction under the chemical conditions employed, and therefore simply represent a non-recoverable loss of NO_2. Moreover, the COF_2 and FNO products do not absorb in the experimental spectral region, and therefore do not complicate the analysis.

$$CF_3 + NO_2 \rightarrow COF_2 + FNO \qquad (11)$$

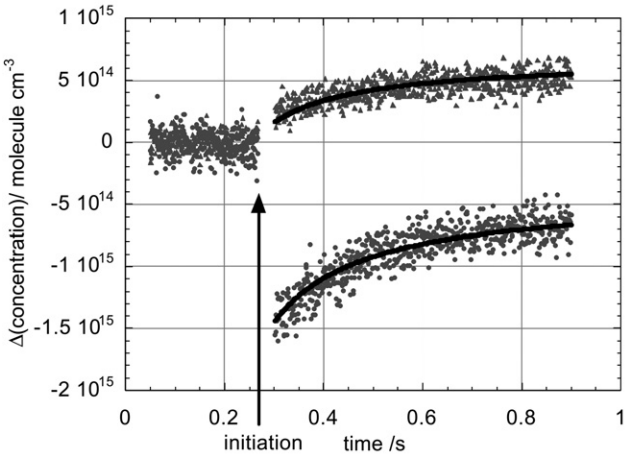

Fig. 5 Temporal evolution of the change in NO_2 concentration (filled circles) and the change in I_2 concentration (filled triangles) in the photolysis of a $NO_2/CF_3I/N_2$ gas mixture. Changes in concentration are calculated relative to pre-photolysis values. Also shown (solid lines) are optimised fits to the NO_2 and I_2 temporal behaviour using a kinetic model constrained to a (2 : 1), (NO_2 : I_2) product stoichiometry.

A minor channel of the CF_3 reaction with NO_2 produces CF_3O and NO:[57]

$$CF_3 + NO_2 \rightarrow CF_3O + NO \qquad (12)$$

The subsequent fate of CF_3O under the experimental conditions chosen is also reaction with NO_2.[59,60] The CF_3O reaction with NO_2 produces primarily CF_3ONO_2, although COF_2 and FNO_2 are also reported to be produced.[59] These (minor) products did not affect the INO_2 recombination chemistry, which was always well-modelled using a 2 : 1 NO_2 : I_2 product formation stoichiometry. Numerical modelling of NO_2 temporal traces, employing the full scheme of secondary chemistry shown in Table 2 was used to extract the rate coefficient for reaction (1). The commercial package FACSIMILE[61] was used to fit simulated to experimental traces, by varying two adjustable model parameters, namely the rate coefficient for reaction (1) and the degree of photolysis of CF_3I. The degree of photolysis of CF_3I essentially controlled the I atom and hence the INO_2 concentration in the model, which in turn controlled the initially lost NO_2 concentration which was simulated for comparison with experiment. Also included in the model was a small contribution to the loss of NO_2 attributed to direct photolysis of NO_2. The magnitude of this contribution was inferred from analysis of experiments performed in the absence of CF_3I, under otherwise identical conditions (but taking account of the different fate of the photolytically generated O atom in the absence and presence of excess CF_3I). A typical NO_2 decay trace and model fit are shown in Fig. 5. A sensitivity analysis was also carried out to confirm that secondary reactions did not affect the returned rate coefficient for reaction (1). This analysis was carried out by successively reanalysing a representative NO_2 decay trace using a model with, in turn, each of the secondary reaction rate coefficients doubled or halved. None of the adjustments to the secondary reaction rate coefficients led to more than a 1% change in the returned value for k_1 from the model fit to the representative trace. Moreover, no systematic variation in k_1 was observed over the range of NO_2 and CF_3I concentrations indicated above.

Reaction (1) was studied over the temperature range 277.7–344.8 K. Rate coefficients for reaction (1) are given in Table 3, and plotted in Arrhenius form in Fig. 6. The temperature dependent rate coefficient is well described by $k_1(T) = (4.7 \pm 0.55) \times 10^{-13} \exp((-1670 \pm 340)/T)$ molecule^{-1} cm^3 s^{-1}, where errors represent 2σ statistical only from the Arrhenius fit. Also shown on Fig. 6 is the single previous determination of k_1 (at 350 K), by van den Bergh and Troe[22] and the current NASA-JPL[62] recommendation for k_1 for atmospheric

Table 2 Reactions used in the FACSIMILE model

Reaction	Rate coefficient/ molecule^{-1} cm^3 s^{-1}	Reference
$I + NO_2$ (+M) $\rightarrow INO_2$ (+M)	7.40×10^{-12} [a]	62
$CF_3 + NO_2 \rightarrow COF_2 + NOF$	1.80×10^{-11}	57,58
$CF_3 + NO_2 \rightarrow CF_3O + NO$	4.80×10^{-12}	57
$CF_3O + NO_2 \rightarrow CF_3ONO_2$	1.65×10^{-11}	59
$CF_3O + NO_2 \rightarrow COF_2 + FNO_2$	3.20×10^{-12}	59
$NO + NO_2$ (+M) $\rightarrow N_2O_3$(+M)	7.60×10^{-15} [a]	63
N_2O_3 (+M) $\rightarrow NO + NO_2$ (+M)	3.60×10^{5} [b]	63
$O + NO_2 \rightarrow NO_3$	2.20×10^{-11}	63
$O + NO_2 \rightarrow NO + O_2$	9.73×10^{-12}	63
$O + CF_3I \rightarrow IO + CF_3$	4.39×10^{-12}	64
$IO + NO_2$ (+M) $\rightarrow IONO_2$ (+M)	1.45×10^{-11} [a]	62
$NO_3 + NO_2 \rightarrow N_2O_5$	1.50×10^{-12}	63
IO + IO $\rightarrow$ products	8.18×10^{-11} [c]	65

[a] At $p = 1$ atm (101 325 Pa). [b] At $p = 1$ atm (101 325 Pa), units s^{-1}. [c] at $T = 296$ K.

Table 3 Rate coefficients for reaction (1)

Temperature/K	$k_1/10^{-15}$ molecule^{-1} cm^3 s^{-1}
277.7	1.13 ± 0.12
285.7	1.42 ± 0.15
303.0	1.50 ± 0.53
312.5	2.11 ± 0.62
322.6	2.66 ± 0.13
333.0	3.70 ± 0.11
344.8	3.65 ± 0.11

k_1 (this work) as $f(T)$. Errors are 2σ.

modelling purposes. The results of this work are at the lower limit of the range of quoted uncertainty on the NASA-JPL recommendation.

The INO_2 kinetics measured here imply that gas phase INO_2 is unlikely to self-react in the atmosphere. On this basis, we speculate that the principal fate of INO_2 formed in the marine boundary layer is likely to be solar photolysis or heterogeneous uptake. Taking a notional maximum volume mixing ratio of INO_2 of 5 pptv, the 298 K rate of loss of INO_2 calculated through reaction (1) is *ca.* 50 molecule cm^{-3} s^{-1}. This loss rate of 5 pptv of INO_2 is equivalent to a first order loss rate with a characteristic rate coefficient of $<10^{-6}$ s^{-1}. Heterogeneous uptake could certainly exceed this rate coefficient, although the $ClNO_2$ uptake coefficient is reported to be small (*ca.* 10^{-6}).[26] By contrast, the preliminary estimates of the INO_2 photolysis rate coefficient (J value) based upon red shifted $ClNO_2$ cross-sections gives $J_{INO_2} \approx 3.84 \times 10^{-4}$ s^{-1} in the Springtime midlatitude marine boundary layer.[43] If this were confirmed, and if heterogeneous uptake of INO_2 was an inefficient process, this J value would imply that solar photolysis is the principal fate of gas phase INO_2 formed in the troposphere. Further spectroscopic investigation of INO_2 in the UV-visible spectral region is clearly warranted.

Conclusions

The first determination of the ambient temperature rate constant for the INO_2 self-reaction along with the first temperature dependence study of this reaction, described by $k_1(T) = (4.7 \pm 0.55) \times 10^{-13} \exp((-1670 \pm 340)/T)$ molecule^{-1} cm^3 s^{-1}, between 277.7 K and 344.8 K, has been carried out.

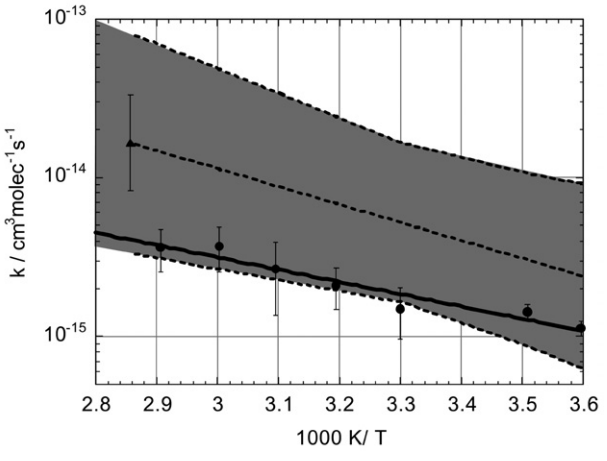

Fig. 6 Arrhenius plot of k_1 obtained in this work (filled circles, error bars are 2σ) and k_1 obtained at 350 K by van den Bergh and Troe (filled triangle).[22] Also shown is the current NASA-JPL recommendation for k_1[62] (dashed line) and the upper and lower bounds of uncertainty on k_1 associated with this recommendation (indicated by the shaded area).

The presence of this reaction was confirmed by monitoring both NO_2 and I_2 products, which showed a 2 : 1 stoichiometric ratio and consistent kinetics. The INO_2 self-reaction is insufficiently rapid to compete with other likely loss channels for atmospheric INO_2.

Acknowledgements

D. M. R. thanks the UK Natural Environment Research Council (NERC) for the award of an Advanced Fellowship. K. S. G. and G. B. thank NERC for the award of postgraduate studentships.

References

1 W. L. Chameides and D. D. Davis, *J. Geophys. Res., [Atmos.]*, 1980, **85**, 7383.
2 M. E. Jenkin, R. A. Cox and D. E. Candeland, *J. Atmos. Chem.*, 1985, **2**, 359.
3 R. B. Chatfield and P. J. Crutzen, *J. Geophys. Res., [Atmos.]*, 1990, **95**, 22 319.
4 M. E. Jenkin, *A Comparative Assessment of the Role of Iodine Photochemistry in Tropospheric Ozone Depletion*, in *The Tropospheric Chemistry of Ozone in the Polar Regions*, eds. H. Niki and K. H. Becker, Springer-Verlag, New York, 1993.
5 D. Davis, J. Crawford, S. Liu, S. McKeen, A. Bandy, D. Thornton, F. S. Rowland and D. Blake, *J. Geophys. Res., [Atmos.]*, 1996, **101**, 2135.
6 S. Solomon, R. R. Garcia and A. R. Ravishankara, *J. Geophys. Res., [Atmos.]*, 1994, **99**, 20 491.
7 P. S. Liss and P. G. Slater, *Nature (London)*, 1974, **247**, 181.
8 R. A. Rasmussen, M. A. K. Khalil, R. Gunawardena and S. D. Hoyt, *J. Geophys. Res., [Atmos.]*, 1982, **87**, 3086.
9 H. B. Singh, L. J. Salas and R. E. Stiles, *J. Geophys. Res., [Atmos.]*, 1983, **88**, 3684.
10 W. Riefenhauser and K. G. Heumann, *Atmos. Environ., Part A*, 1992, **26**, 2905.
11 Th. Class and K. Ballschmiter, *J. Atmos. Chem.*, 1988, **6**, 35.
12 C. Schall and K. G. Heumann, *Fresnius J. Anal. Chem.*, 1993, **346**, 717.
13 L. J. Carpenter, W. T. Sturges, S. A. Penkett, P. S. Liss, B. Alkie, K. Hebestreit and U. Platt, *J. Geophys. Res., [Atmos.]*, 1999, **104**, 1679.
14 S. W. Benson, *Thermochemical Kinetics*, John Wiley & Sons, New York, 1973.
15 M. E. Jenkin, R. A. Cox, A. Mellouki, G. LeBras and G. Poulet, *J. Phys. Chem.*, 1990, **94**, 2927.
16 F. Maguin, G. Laverdet, G. LeBras and G. Poulet, *J. Phys. Chem.*, 1992, **96**, 1775.
17 M. E. Jenkin, R. A. Cox and G. D. Hayman, *Chem. Phys. Lett.*, 1991, **177**, 272.
18 E. P. Daykin and P. H. Wine, *J. Phys. Chem.*, 1990, **94**, 4528.
19 D. M. Rowley, J. C. Mossinger, R. A. Cox and R. L. Jones, *J. Atmos. Chem.*, 1999, **34**, 137.
20 D. Bauer, T. Ingham, S. A. Carl, G. K. Moortgat and J. N. Crowley, *J. Phys. Chem. A*, 1998, **102**, 2857.
21 J. C. Mossinger, D. M. Rowley and R. A. Cox, *Atmos. Chem. Phys.*, 2002, **2**, 227.
22 H. van den Bergh and J. Troe, *J. Chem. Phys.*, 1976, **64**, 736.
23 J. V. Seeley, J. T. Jayne and M. J. Molina, *J. Phys. Chem.*, 1996, **100**, 4019.
24 A. Mellouki, G. Laverdet, J. L. Jourdain and G. Poulet, *Int. J. Chem. Kinet.*, 1989, **21**, 1161.
25 K. D. Kreutter, J. M. Nicovich and P. H. Wine, *J. Phys. Chem.*, 1991, **95**, 4020.
26 W. Behnke, C. George, V. Scheer and C. Zetzsch, *J. Geophys. Res., [Atmos.]*, 1997, **102**, 3795.
27 B. J. Finlayson-Pitts, F. E. Livingston and H. N. Berko, *J. Phys. Chem.*, 1989, **93**, 4397.
28 D. R. Hanson and A. R. Ravishankara, *J. Phys. Chem.*, 1992, **96**, 9441.
29 R. Karlsson and E. Ljungstrom, *Atmos. Environ.*, 1998, **32**, 1711.
30 T. J. Lee, *J. Phys. Chem.*, 1994, **98**, 111.
31 J. Orphal, M. Morillon-Chapey, S. Klee, G. C. Mellau and M. Winnewisser, *J. Mol. Spectrosc.*, 1998, **190**, 101.
32 J. Orphal, A. Frenzel, H. Grothe, B. Redlich, D. Scheffler, H. Willner and C. Zetzsch, *J. Mol. Spectrosc.*, 1998, **191**, 88.

33 T. J. Lee, *J. Phys. Chem.*, 1996, **100**, 19 847.
34 J. A. Ganske, H. N. Berko and B. J. Finlayson-Pitts, *J. Geophys. Res., [Atmos.]*, 1992, **97**, 7651.
35 H. H. Nelson and H. S. Johnston, *J. Phys. Chem.*, 1981, **85**, 3891.
36 J. M. Coanga, L. Schriver-Mazzuoli, A. Schriver and P. R. Dahoo, *Chem. Phys.*, 2002, **276**, 309.
37 J. B. Burkholder and J. J. Orlando, *Chem. Phys. Lett.*, 2000, **317**, 603.
38 D. E. Tevault, *J. Phys. Chem.*, 1979, **83**, 2217.
39 J. J. Orlando and J. B. Burkholder, *J. Phys. Chem.*, 2000, **104**, 2048.
40 H. T. Yu, Y. J. Chi, H. G. Fu, X. R. Huang, Z. S. Li and J. Z. Sun, *Chin. Chem. Lett.*, 2002, **13**, 1138.
41 I. Barnes, K. H. Becker and J. Starcke, *J. Phys. Chem.*, 1991, **95**, 9736.
42 M. Feuerhahn, R. Minkwitz and U. Engelhardt, *J. Mol. Spectrosc.*, 1979, **77**, 429.
43 J. Stutz, K. Hebestreit, B. Alicke and U. Platt, *J. Atmos. Chem.*, 1999, **34**, 65.
44 R. T. Carter, A. Hallou and J. R. Huber, *Chem. Phys. Lett.*, 1999, **310**, 166.
45 A. Furlan, M. A. Haeberli and J. R. Huber, *J. Phys. Chem.*, 2000, **104**, 10 392.
46 J. Zhu, Z. X. Cao and Q. F. Zhang, *Huaxue Xuebao*, 2002, **60**, 1040.
47 R. A. Wilkins, Jr., M. C. Dodge and I. C. Hisatsune, *J. Phys. Chem.*, 1974, **78**, 2073.
48 J. A. Ganske, H. N. Berko, M. J. Ezell and B. J. Finlayson-Pitts, *J. Phys. Chem.*, 1992, **96**, 2568.
49 R. Broske and F. Zabel, *J. Phys. Chem. A*, 1998, **102**, 8626.
50 R. Vogt, R. Sander, R. Von Glasow and P. J. Crutzen, *J. Atmos. Chem.*, 1999, **32**, 375.
51 S. N. Buben, I. K. Larin, N. A. Messineva and E. M. Trofimova, *Kinet. Catal.*, 1990, **31**, 854.
52 C. J. Cobos and J. Troe, *J. Chem. Phys.*, 1985, **83**, 1010.
53 H. van den Bergh, N. Benoit-Guyot and J. Troe, *Int. J. Chem. Kinet.*, 1977, **9**, 223.
54 D. M. Rowley, M. H. Harwood, R. A. Freshwater and R. L. Jones, *J. Phys. Chem.*, 1996, **100**, 3020.
55 M. H. Harwood and R. L. Jones, *J. Geophys. Res., [Atmos.]*, 1994, **99**, 22 955.
56 J. Tellinghuisen, *J. Chem. Phys.*, 1973, **58**, 2821.
57 J. Sehested, O. J. Nielsen, C. A. Rinaldi, S. I. Lane and J. C. Ferrero, *Int. J. Chem. Kinet.*, 1996, **28**, 579.
58 K. W. Oum and G. Hancock, *J. Phys. Chem. A*, 1997, **101**, 2634.
59 F. Caralp, M.-T. Rayez, W. Forst, C. Bourbon, M. Brioukov and P. Devolder, *J. Chem. Soc., Faraday Trans.*, 1997, **93**, 3751.
60 C. Fockenberg, H. Somnitz, G. Bednarek and R. Zellner, *Ber. Bunsen-Ges. Phys. Chem.*, 1997, **101**, 1411.
61 A. R. Curtis and W. P. Sweetenham, FACSIMILE, AERE Harwell publication R 12805, Computer Science and System Division, Harwell Laboratory, Oxfordshire, UK, 1987.
62 W. B. DeMore, S. P. Sander, D. M. Golden, R. F. Hampson, M. J. Kurylo, C. J. Howard, A. R. Ravishankara, C. E. Kolb and M. J. Molina, *Chemical Kinetics and Photochemical Data for Use in Stratospheric Modelling*, JPL Publication 97-4, Jet Propulsion Laboratory, Pasadena, CA, 1997.
63 R. Atkinson, D. L. Baulch, R. A. Cox, R. F. Hampson, Jr., J. A. Kerr, M. J. Rossi and J. Troe, Evaluated kinetic and photochemical data for atmospheric chemistry: supplement VI. IUPAC subcommittee on gas kinetic data evaluation for atmospheric chemistry, *J. Phys. Chem. Ref. Data*, 1997, **26**, 1329.
64 M. K. Gilles, A. A. Turnipseed, R. K. Talukdar, Y. Rudich, Y. P. W. Villalta, L. G. Huey, J. B. Burkholder and A. R. Ravishankara, *J. Phys. Chem.*, 1996, **100**, 14 005.
65 W. J. Bloss, D. M. Rowley, R. A. Cox and R. L. Jones, *J. Phys. Chem. A.*, 2001, **105**, 7840.